Title

Stochastic Constrained Extended System Dynamics for Solving Charge Equilibration Models.

Journal

Journal of Chemical Theory and Computation, 16(10)

ISSN

1549-9618

Authors

Tan, Songchen
Leven, Itai
An, Dong
et al.

Publication Date

2020-10-13

DOI

10.1021/acs.jctc.0c00514

Peer reviewed

Stochastic Constrained Extended System Dynamics for Solving Charge Equilibration Models

Songchen Tan[1,2], Itai Leven[2,3],Dong An[4,5], Lin Lin[4,5], Teresa Head-Gordon[2,3,6*,†]

†[1] *College of Chemistry and Molecular Engineering, Peking University, China*

‡[2] *Kenneth S. Pitzer Theory Center, University of California, Berkeley, CA, USA*

¶[3] *Chemical Sciences, Lawrence Berkeley National Laboratory, Berkeley, CA, USA*

§[4] *Department of Mathematics, University of California, Berkeley, CA, USA*

‖[5] *Computational Research, Lawrence Berkeley National Laboratory, Berkeley, CA, USA*

⊥[6] *Departments of Chemistry, Bioengineering, and Chemical and Biomolecular Engineering, University of California, Berkeley, CA, USA,*

E-mail: thg@berkeley.edu

Abstract

We present a new stochastic extended Lagrangian molecular dynamics solution to charge equilibration that eliminates self-consistent field (SCF) calculations, thus eliminating the computational bottleneck in solving the charge distribution with standard SCF solvers. By formulating both charges and chemical potential as latent variables, and introducing a holonomic constraint that satisfies charge conservation, the SC-XLMD method accurately reproduces thermodynamic, dynamic and structural properties within the framework of ReaxFF for a bulk water system and a highly reactive RDX molecules simulated at high temperature. The SC-XLMD method shows excellent computational performance and is available in the publicly available LAMMPS package.

1 Introduction

Many non-reactive and reactive force fields have relied on the electronegativity equalization method[1,2] (EEM) or charge equilibration model[3] (CEM) to describe charge flow in and between molecules. The EEM was inspired by the concepts of atomic electronegativity and hardness drawn from Density Functional Theory[4] to define an electrostatic model that allows the charges on atoms to fluctuate with changing nuclear configurations during molecular simulations.[1,2] The EEM was later generalized to the CEM by Rappe and Goddard to include a screened electrostatic interaction between charges, using empirical atomic parameters such as ionization potentials, electron affinities, and atomic radii to parameterize the model.[3] The CEM has been successfully applied to a variety of chemical systems such as proteins[5] and membranes,[6] metal-organic frameworks,[7,8] and to describe the quartz-stishovite phase transition.[9]

The rate limiting step of the CEM is the determination of new charge distribution from two sets of linear equations, which represent the minimization of the total energy for the new nuclear configuration under a constraint that the total charge of the system is conserved. This may be solved directly for small systems (typically with Cholesky decomposition), but must be solved iteratively in practice for large systems using solvers such as the direct inversion in the iterative subspace (DIIS)[10] or conjugate gradient (CG) methods.[11] The number of self-consistent field (SCF) iterations can be reduced with careful preconditioning, polynomial extrapolation from previous steps, and good software implementations,[12–14] but solving new charge distributions at each time step remains the most computationally demanding component of MD simulations using ReaxFF,[15] which is often one order of magnitude slower than traditional non-reactive force fields. Recently we have also been aware of several optimizations[16,17] in terms of preconditioners such as the sparse approximate inverse (SAI) preconditioner, as well as communication overheads through multicore architectures. While these optimizations can reduce the iteration number to 5 ~20 (10^{-10} criteria), they may require prior knowledge about simulation systems to configure the *ad hoc* optimization

techniques.

An alternative approach is to formulate an extended system of auxiliary electronic variables that are evolved in time with extended Lagrangian molecular dynamics (XLMD).[18–21] With an extended Lagrangian that includes fictitious kinetic energy of auxiliary charges, as well as a potential energy that keeps the auxiliary charges close to the exact solution, the extended system are evolved dynamically using symplectic and time-reversible algorithms to replace the iterative solution in determining new charge distributions. Relevant to CEM, Leven and Head-Gordon have recently utilized the dynamically evolved auxiliary charges as an initial guess for the CG method, thereby allowing for a more loose convergence tolerance for final charges without introducing additional (and sometimes even with diminishing) energy drift which measures the stability and accuracy of MD simulations.[21] The resulting inertial extended Lagrangian SCF (iEL/SCF) method was shown to successfully reduce the number of SCF iterations by half or more in the CEM solutions.[15,21]

In this work we further extend the iEL/SCF method for CEM by eliminating SCF cycles altogether, as we have done previously for non-reactive polarizable force fields using iEL/0-SCF.[20,22] For polarizable force fields, the auxiliary induced dipoles evolve under a harmonic potential that keeps their values close to the converged real dipole solution, as approximated by a one-time step estimation derived from a local-kernel mixing of the real and auxiliary variables using an optimal mixing parameter γ. This SCF-free approximation works well if the real dipole dynamics evolve on a longer timescale, well-separated from the discretized time step, so that a local-kernel mixing remains a good approximation to the true SCF solution. Another important consideration in the iEL/0-SCF method is to control the problems of resonance, i.e. errors in the time-integration of the harmonic forces that leak to the auxiliary kinetic energy and create numerical instabilities. The resonance problems can be controlled through a separate thermostat for the auxiliary variables as we have shown previously.[20,22] Recently, An and co-workers have developed a new formulation of an iteration-free scheme, Stochastic-XLMD, where a thermostat coupling parameter ε replaces

the mixing parameter γ, and the effect of a Langevin thermostat applied to the latent induced dipole variables for classical polarization was shown to be robust, although not strictly time-reversible.[22]

However, the generalization of the resulting iEL/0-SCF or Stochastic-XLMD methods from induced dipoles to fluctuating charges is not straightforward for three reasons: (1) the characteristic decorrelation time for charges is more than one order of magnitude faster than for induced dipoles, (2) the charges are derived under a constraint that the total charge of the entire system is conserved, and (3) the resonance problem may be more severe under a harmonic potential now applied to two sets of coupled linear equations. To illustrate, an iteration-free XLMD scheme for CEM,[23,24] was found to be unstable in a trajectory of no more than several picoseconds,[21] which is generally not sufficient for converging thermodynamic quantities.

In this work, we have addressed these issues through careful formulation of an XLMD procedure that utilizes two types of latent variables - the charge and chemical potential - and enforces the conservation of charge through a holonomic constraint scheme that is conforming for both energy and forces.[25] We have combined this new SCF-less solution for CEM with the Stochastic-XLMD (SXLMD) method for thermostatting,[22] and implemented it within the ReaxFF force field in the Large-scale Atomic and Molecular Massive Parallel Simulation (LAMMPS) package.[26] We have shown that this stochastic constrained extended Lagrangian scheme with no iteration, SC-XLMD, is capable of producing stable trajectories over a timescale of nanoseconds, while retaining energy conservation and thermodynamics properties compared to the CG method. Compared to the standard implementation in LAMMPS, the computational speed of the new SC-XLMD approach is comparable to a fixed charge calculation, and scales well with increasing number of cores or increasing size of systems.

2 Theory

Charge Equilibration Equation. A general form of the Hamiltonian for the CEM is

$$H = \frac{1}{2}\boldsymbol{p}^T \boldsymbol{M}^{-1}\boldsymbol{p} + U(\boldsymbol{r}) + V(\boldsymbol{r}, \boldsymbol{q}) \tag{1}$$

where $\boldsymbol{r} \in \mathbb{R}^{3n}$ and $\boldsymbol{p} \in \mathbb{R}^{3n}$ are the atom positions and momenta, $\boldsymbol{M} = \text{diag}\{m_1\boldsymbol{I}_3, \cdots, m_n\boldsymbol{I}_3\}$ are the atom mass (diagonal) matrix, $U(\boldsymbol{r})$ encompasses molecular interactions other than the many-body electrostatic potential, $V(\boldsymbol{r}, \boldsymbol{q})$,

$$V(\boldsymbol{r}, \boldsymbol{q}) = \frac{1}{2}\boldsymbol{q}^T \boldsymbol{J}(\boldsymbol{r})\boldsymbol{q} + \boldsymbol{\chi}^T \boldsymbol{q} \tag{2}$$

which is the focus of this work. The potential term in Eq. (2) describes changes in the charges $\boldsymbol{q}$ that are dependent on the electronegativity of atoms when bearing zero charge, $\boldsymbol{\chi}$, and the shielded electrostatic interaction matrix, $\boldsymbol{J}$, comprised of the following matrix elements

$$J_{ij} = \delta_{ij}\eta_i + (1 - \delta_{ij})(r_{ij}^3 + \gamma_{ij}^{-3})^{-1/3} \tag{3}$$

where η_i is related to the atomic hardness, γ_{ij} is the electrostatic screening parameter, and r_{ij} is the distance between atoms i and j.

The CEM allows the charges to rearrange according to the minimization of $V(\boldsymbol{r}, \boldsymbol{q})$ as a response to the motion of atoms, while enforcing the constraint that the total charge remains constant (without loss of generality, we assume the total charge is 0 henceforth):

$$\begin{aligned} L(\boldsymbol{r}, \boldsymbol{q}, \mu) &= V(\boldsymbol{r}, \boldsymbol{q}) - \mu \mathbf{1}^T \boldsymbol{q} \\ &= \frac{1}{2}\boldsymbol{q}^T \boldsymbol{J}(\boldsymbol{r})\boldsymbol{q} + \boldsymbol{\chi}^T \boldsymbol{q} - \mu \mathbf{1}^T \boldsymbol{q} \end{aligned} \tag{4}$$

and

$$\frac{\partial L}{\partial \boldsymbol{q}} = 0 \qquad \frac{\partial L}{\partial \mu} = 0 \tag{5}$$

where the Lagrange multiplier μ is the chemical potential. This yields an $n+1$-dimensional equation:

$$\begin{pmatrix} \boldsymbol{J} & -\mathbf{1} \\ -\mathbf{1} & 0 \end{pmatrix} \begin{pmatrix} \boldsymbol{q} \\ \mu \end{pmatrix} = \begin{pmatrix} -\boldsymbol{\chi} \\ 0 \end{pmatrix} \tag{6}$$

Since a direct inversion of this matrix is prohibitive in practice, Eq. (6) is instead solved by partitioning the original charges $\boldsymbol{q}$ into fictitious charges $\boldsymbol{s}$ and $\boldsymbol{t}$, i.e. $\boldsymbol{q} = \boldsymbol{s} - \mu\boldsymbol{t}$, and then solving $\boldsymbol{J}\boldsymbol{s} = -\boldsymbol{\chi}$ and $\boldsymbol{J}\boldsymbol{t} = -\mathbf{1}$ iteratively with the CG method.[13] The number of iterations can be reduced with careful preconditioning, as well as polynomial extrapolation from previous steps, but the overall computational cost is still significantly larger than conventional simulations using fixed charges, and defines the rate limiting step for reactive force field simulations of large systems.

Extended System Dynamics: the SC-XLMD Method. An alternative solution to the charge equilibration is to formulate an extended system by introducing latent variables that evolve in time with the real degrees of freedom using an XLMD algorithm, as shown in many previous studies.[18–20] However, to the best of our knowledge, there is no known example of successfully treating the charge conservation constraint and the time-evolution consistently for the case of fluctuating charges.

One class of XLMD approach[24,27] is to assign latent momenta $\boldsymbol{p}_q$ and latent mass $\boldsymbol{M}_q = m_q\boldsymbol{I}_n$ to the corresponding $\boldsymbol{q}$ variables, and utilizing a Hamiltonian of the form

$$\begin{aligned} H^{(1)}_{\text{ext}}(\boldsymbol{r},\boldsymbol{p},\boldsymbol{q},\boldsymbol{p}_q) = &\frac{1}{2}\boldsymbol{p}^T\boldsymbol{M}^{-1}\boldsymbol{p} + \frac{1}{2}\boldsymbol{p}_q^T\boldsymbol{M}_q^{-1}\boldsymbol{p}_q \\ &+ U(\boldsymbol{r}) + V(\boldsymbol{r},\boldsymbol{q}) \end{aligned} \tag{7}$$

This XLMD approach completely ignores any constraint and thus will exhibit significant problems with charge conservation in a long simulation.

The second class of XLMD method,[23,28] utilizes a Hamiltonian that is equivalent to

$$\begin{aligned} H^{(2)}_{\text{ext}}(\boldsymbol{r},\boldsymbol{p},\boldsymbol{q},\boldsymbol{p}_q) = \frac{1}{2}\boldsymbol{p}^T\boldsymbol{M}^{-1}\boldsymbol{p} + \frac{1}{2}\boldsymbol{p}_q^T\boldsymbol{M}_q^{-1}\boldsymbol{p}_q \\ + U(\boldsymbol{r}) + V(\boldsymbol{r},\boldsymbol{q}) - \mu\mathbf{1}^T\boldsymbol{q} \end{aligned} \tag{8}$$

where $\mu = \mu(\boldsymbol{r},\boldsymbol{q})$ is determined on-the-fly by solving the following algebraic equation every time step,

$$\mathbf{1}^T(\boldsymbol{J}\boldsymbol{q} + \boldsymbol{\chi} - \mu\mathbf{1}) = 0 \tag{9}$$

However, the resulting differential-algebraic system is non-Hamiltonian and is vulnerable to numerical noise. As a result, both of these classes of XLMD methods have not been able to perform a simulation for CEM longer than 10 ps, which is generally not enough for converging thermodynamic quantities.

Here instead, we consider a new extended Hamiltonian in which we treat the charges $\boldsymbol{q}$ and chemical potential μ together as an extended set of latent positions, $\boldsymbol{l} = (\boldsymbol{q},\mu)$ with latent momenta $\boldsymbol{p}_l = (\boldsymbol{p}_q, p_\mu)$ as well as latent mass $\boldsymbol{M}_l = \text{diag}\{m_q\boldsymbol{I}_n, m_\mu\}$

$$\begin{aligned} H^{(3)}_{\text{ext}}(\boldsymbol{r},\boldsymbol{p},\boldsymbol{l},\boldsymbol{p}_l) = \frac{1}{2}\boldsymbol{p}^T\boldsymbol{M}^{-1}\boldsymbol{p} + \frac{1}{2}\boldsymbol{p}_l^T\boldsymbol{M}_l^{-1}\boldsymbol{p}_l \\ + U(\boldsymbol{r}) + \frac{1}{2}\boldsymbol{l}^T\boldsymbol{A}(\boldsymbol{r})\boldsymbol{l} - \boldsymbol{b}^T\boldsymbol{l} \end{aligned} \tag{10}$$

where

$$\boldsymbol{A}(\boldsymbol{r}) = \begin{pmatrix} \boldsymbol{J}(\boldsymbol{r}) & -\mathbf{1} \\ -\mathbf{1} & 0 \end{pmatrix} \quad \boldsymbol{b} = \begin{pmatrix} -\boldsymbol{\chi} \\ 0 \end{pmatrix} \tag{11}$$

Since the many-body potential term in $H^{(3)}_{\text{ext}}$ is exactly what is minimized in the Lagrange multiplier method, the evolution of the latent variables will consistently keep close to the Born-Oppenheimer energy surface, as well as keeping the total charge constant. Furthermore, by making connections to the well-known holonomic constraint scheme in classical molecular

dynamics,[25] we can define a function $\boldsymbol{z}(\boldsymbol{l})$ of the latent variables described as a projection,

$$\boldsymbol{z}(\boldsymbol{l}) = \begin{pmatrix} \boldsymbol{I}_n - \mathbf{1}\mathbf{1}^T/n & 0 \\ 0 & 1 \end{pmatrix} \boldsymbol{l} \tag{12}$$

By replacing $\boldsymbol{l}$ in $H_{\text{ext}}^{(3)}$ with $\boldsymbol{z}(\boldsymbol{l})$, we arrive at our final expression of the extended Hamiltonian used in this work:

$$\begin{aligned} H_{\text{ext}}(\boldsymbol{r}, \boldsymbol{p}, \boldsymbol{l}, \boldsymbol{p}_l) = \frac{1}{2}\boldsymbol{p}^T \boldsymbol{M}^{-1}\boldsymbol{p} + \frac{1}{2}\boldsymbol{p}_l^T \boldsymbol{M}_l^{-1}\boldsymbol{p}_l \\ + U(\boldsymbol{r}) + \frac{1}{2}\boldsymbol{z}^T(\boldsymbol{l})\boldsymbol{A}(\boldsymbol{r})\boldsymbol{z}(\boldsymbol{l}) - \boldsymbol{b}^T\boldsymbol{z}(\boldsymbol{l}) \end{aligned} \tag{13}$$

We note that when we derive the latent force from H_{ext}, we obtain

$$\dot{\boldsymbol{p}}_l = -\frac{\partial H_{\text{ext}}}{\partial \boldsymbol{l}} = \begin{pmatrix} \boldsymbol{I}_n - \mathbf{1}\mathbf{1}^T/n & 0 \\ 0 & 1 \end{pmatrix} (\boldsymbol{b} - \boldsymbol{A}\boldsymbol{z}) \tag{14}$$

which satisfies $\mathbf{1}^T\dot{\boldsymbol{p}}_q = 0$. Therefore, with proper initialization of the latent position and momenta that satisfies $\mathbf{1}^T\boldsymbol{q}(0) = \mathbf{1}^T\boldsymbol{p}_q(0) = 0$, the time evolution keeps $\mathbf{1}^T\boldsymbol{q}(t) = 0$ for arbitrary t. We note that implementing this constraint does not disturb the symplectic structure of integration, which is beneficial for long time stable simulation.[25]

3 Methods

Langevin Thermostat and Integration Algorithm. We utilize the Langevin thermostat approach we have developed previously for thermostating polarizable models,[22] which requires us to define both dissipation $\boldsymbol{\Gamma}_l = \text{diag}\{\gamma_q \boldsymbol{I}_n, \gamma_\mu\}$ and temperature $\boldsymbol{T}_l = \text{diag}\{T_q \boldsymbol{I}_n, T_\mu\}$ parameters corresponding to the latent variables. Once defined, the "BAOAB" scheme is used to achieve efficient thermostatting[29] by propagating the equations of the extended system as follows:

- Step B for $\Delta t/2$:

$$\boldsymbol{p} \leftarrow \boldsymbol{p} - \frac{\partial H_{\text{ext}}}{\partial \boldsymbol{r}} \frac{\Delta t}{2}$$

$$\boldsymbol{p}_l \leftarrow \boldsymbol{p}_l - \frac{\partial H_{\text{ext}}}{\partial \boldsymbol{l}} \frac{\Delta t}{2}$$

- Step A for $\Delta t/2$:

$$\boldsymbol{r} \leftarrow \boldsymbol{r} + \boldsymbol{M}^{-1}\boldsymbol{p} \frac{\Delta t}{2}$$

$$\boldsymbol{l} \leftarrow \boldsymbol{l} + \boldsymbol{M}_l^{-1}\boldsymbol{p}_l \frac{\Delta t}{2}$$

- Step O for Δt;
- Step A for $\Delta t/2$;
- Step B for $\Delta t/2$;

Additional details to enforce the charge constraint in the Step O are provided in Appendix A. The benefit of this scheme was shown in our previous work that proved that the trajectory of the extended system will converge to the real system when $\boldsymbol{M}_l \to 0$ for arbitrary initial condition of latent variable $\boldsymbol{l}$.[22]

Having formulated the integration algorithm with thermostats, we now explain the rationale to determine the parameters. We first note that for a one-dimensional harmonic oscillator with force constant k and mass m, a stable numerical integration should satisfy $\Delta t^2 k/m = \Delta t^2 \omega^2 < 2$.[30] For the CEM model, the "force constant" is $\boldsymbol{J}(\boldsymbol{r})$, thus it is subject to

$$\Delta t^2 \rho(\boldsymbol{J}(\boldsymbol{r})) m_q^{-1} < 2 \tag{15}$$

where $\rho(\boldsymbol{J}(\boldsymbol{r}))$ denotes the maximum absolute value of the eigenvalues of $\boldsymbol{J}(\boldsymbol{r})$, which is approximately the inverse of the minimum atom hardness, η_{min}^{-1}. The above equation in turn determines the mass by

$$m_q > m_{q,\text{min}} = \frac{\Delta t^2}{2\eta_{\text{min}}} \tag{16}$$

In practice, we will use $m_q = 5m_{q,\min}$ throughout the paper to ensure a stable trajectory.

The choice of charge temperature T_q is determined by taking derivatives on both sides of the charge equilibration equation:

$$\begin{pmatrix} \dot{\boldsymbol{J}} & \mathbf{0} \\ \mathbf{0} & 0 \end{pmatrix} \boldsymbol{l} + \begin{pmatrix} \boldsymbol{J} & -\mathbf{1} \\ -\mathbf{1} & 0 \end{pmatrix} \dot{\boldsymbol{l}} = \begin{pmatrix} 0 \\ 0 \end{pmatrix} \tag{17}$$

where the derivative of $\boldsymbol{J}$ can be easily calculated by noticing $J_{ij} = f(r_{ij})$, and

$$\frac{\mathrm{d}r_{ij}}{\mathrm{d}t} = \sum_{\alpha=x,y,z} \frac{(r_{i\alpha} - r_{j\alpha})(v_{i\alpha} - v_{j\alpha})}{r_{ij}} \tag{18}$$

so that

$$\dot{J}_{ij} = \frac{f'(r_{ij})}{r_{ij}} \sum_{\alpha=x,y,z} (r_{i\alpha} - r_{j\alpha})(v_{i\alpha} - v_{j\alpha}) \tag{19}$$

In practice, short exact trajectories using a tight convergence (10^{-12}) is calculated and the derivatives of charges are collected. Next, we view this as the "intrinsic motion" of charges and calculate their averaged intrinsic velocity. Then, from the averaged intrinsic velocity and latent mass we obtained the appropriate latent temperature T_q:

$$T_q = \frac{1}{2} m_q \langle \dot{\boldsymbol{q}}^T \dot{\boldsymbol{q}} \rangle / n \tag{20}$$

Generally, the more reactive the system is, the faster the charges are fluctuating, and the higher the latent temperature is.

In regards the parameters related to chemical potential, i.e. $(m_\mu, \gamma_\mu, T_\mu)$, we note that in practice the initial velocity $\dot{\mu}$ solved from the above equations were found to be negligible, so we assign $\dot{\mu}(0) = 0$, then μ will be a constant of motion, thus we no longer need to determine them.

Simulation Methods. We have implemented SC-XLMD within the framework of the LAMMPS software package[26] for ReaxFF.[15] We use a cubic box comprising 233 water

molecules, for which the force field developed by Rahaman *et al* is used,[31] as well as a cubic box comprising 40 RDX molecules with the force field developed by Shan *et al.*[32] For all NVE simulations, the system is first equilibrated in the NVT ensemble (with Nosé-Hoover thermostats[33]) at the desired temperature for 10 ps, followed by NVE propagation for 500 ps and up to 5 ns for water. To measure hydronium diffusion, the system is prepared by adding one proton to the previously described water system of 233 water molecules, which corresponds to a 0.2 M aqueous solution of a strong acid such as HCl. For all NVT simulations the real system variables are also thermostatted with a 4th-order Nosé-Hoover chain[33] along with the thermostat applied to the latent variables, and statistics collected over 500 ps. The water system was characterized at 300 K and the RDX system at 300 K and 1000 K. A time step of $\Delta t = 0.15$ fs was used in all simulations at 300 K as suggested by previous work[23] except for the RDX system at 1000 K, which required a timestep of $\Delta t = 0.10$ fs.

4 Results

Energy Conservation and Latent Temperature. The conservation of the total energy is the most important intrinsic indicator of correct dynamics for any molecular dynamics algorithm. We note that energy conservation for ReaxFF in LAMMPS may be poor due to discontinuities in the potential energy surface, which has been identified to arise from distance cut-offs of the bond order terms.[34] Nonetheless we take the CG method with a 10^{-10} convergence criteria as the gold standard for energy conservation comparison. We also consider an XLMD method which uses no latent variable thermostats of the extended system Hamiltonian (C-XLMD), and compare it against the complete SC-XLMD solution which uses Langevin thermostats. As shown in Figure 1a, there is no more loss of energy conservation for C-XLMD (i.e. with no thermostat coupling $\gamma_q = 0$) as compared to the CG method. However the latent variables are susceptible to numerical noise because of integrator resonance,[20,22] and without dissipation, the numerical error will accumulate and cause

the kinetic energy of latent variables to increase as shown in Figure 1b.

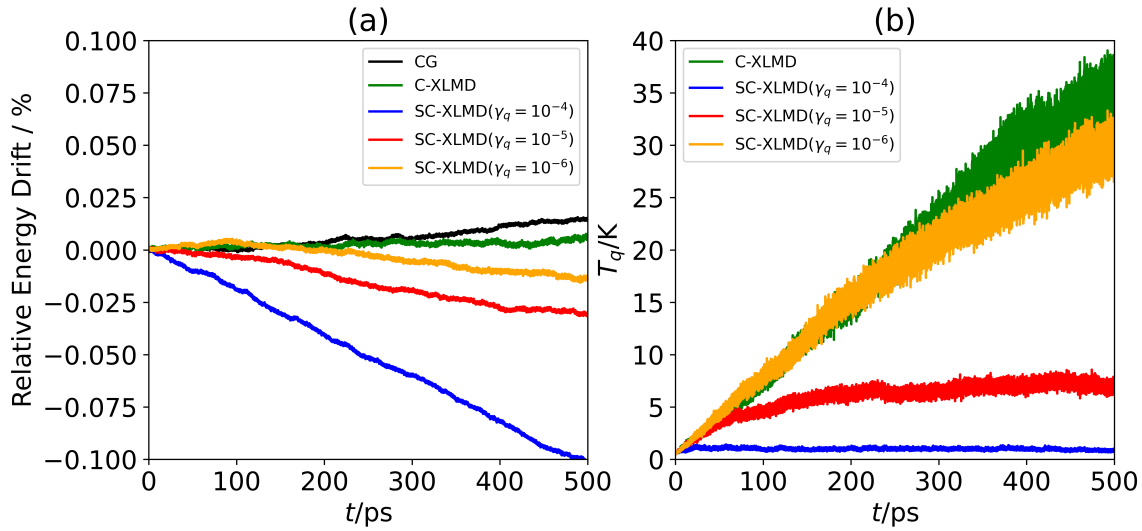

Figure 1: Comparison of methods for energy conservation and latent charge temperature of the CEM simulation for bulk water. (a) Total relative energy drift in percentage units as a function of time for CG (10^{-10} convergence criteria), an extended Lagrangian with no latent variable thermostatting (C-XLMD), and when using SC-XLMD with various values of the latent thermostat coupling parameter γ_q. The absolute value of energy drift rates in percent ns^{-1} are 0.03 (CG), 0.01 (C-XLMD), 0.22 (SC-XLMD with $\gamma_q = 10^{-4}$), 0.05 ($\gamma_q = 10^{-5}$) and 0.03 ($\gamma_q = 10^{-6}$). (b) The corresponding latent charge temperature as a function of time for the above methods except CG.

The resonance effects will eventually cause degradation of the molecular dynamics that will in turn effect physical observables, which we illustrate further below. Hence we require some type of thermostatting of the latent variables at an intrinsically cold temperature to dissipate the error. We thus implemented a Langevin thermostat to control the latent variable temperature, but this requires an optimization of the thermostat coupling parameter for SC-XLMD, and in Figure 1 we have considered values of $\gamma_q = 10^{-4}$, 10^{-5} and 10^{-6}. If $\gamma_q = 10^{-4}$, the charge temperature T_q is very stable, but the energy conservation is severely compromised with respect to CG and C-XLMD. On the other hand, if $\gamma_q = 10^{-6}$, the energy conservation is very good but the charge temperature T_q will increase over time and properties will be compromised.

We therefore suggest that by using $\gamma_q = 10^{-5}$, the energy conservation is comparable

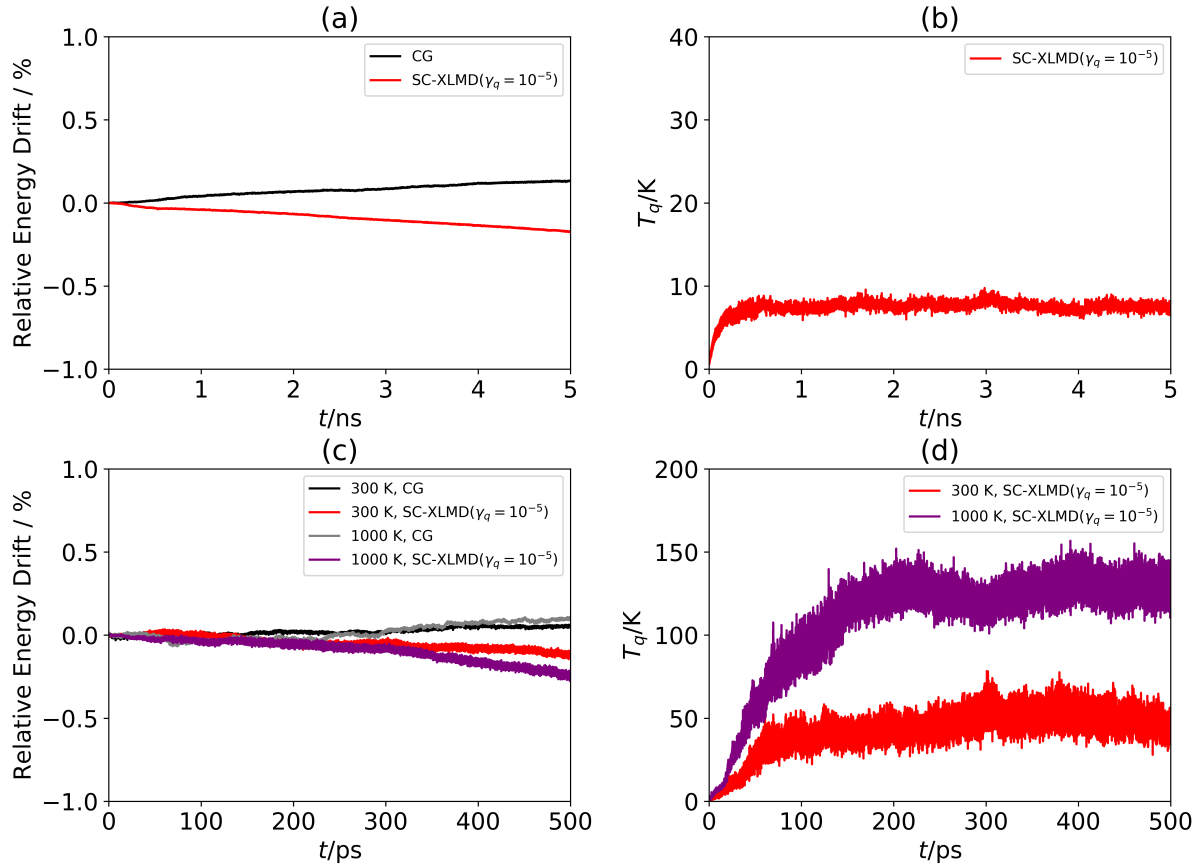

Figure 2: Comparison of SC-XLMD and CG for energy conservation and latent charge temperature of the CEM simulation for water and RDX. (a) Total relative energy drift in percentage units and (b) the corresponding latent charge temperature for SC-XLMD over a 5 ns simulation for water (c) Total relative energy drift in percentage units at 300 K and 1000 K and (d) the corresponding latent charge temperatures as a function of time for RDX. The CG-SCF uses a (10^{-10}) convergence criteria and we compare to the optimal value of $\gamma_q = 10^{-5}$ for the SC-XLMD method.

to the CG method and the latent charge temperature is also kept under good control. To support that this choice of γ_q is reasonably universal, Figure 2 shows that $\gamma_q = 10^{-5}$ is both sufficient for energy conservation and controlling resonance over longer timescales of 5 ns for water, and completely transferable to the RDX system at both 300 K and 1000 K.

Fluctuating Charge Properties. Next, we assess the ability of C-XLMD and SC-XLMD to produce a similar behavior in the converged real charges compared to CG, which is the key feature of all CEM-based simulations and underlies all the calculated physical properties of any system. We examine the real charge distribution (a statistic property) as well as the

charge autocorrelation function (a dynamic property) defined by

$$C_q(t) = \frac{\langle (q(t) - \bar{q})(q(0) - \bar{q}) \rangle}{\langle (q(0) - \bar{q})^2 \rangle}$$
$$\tilde{C}_q(\omega) = \int_0^\infty e^{-i\omega t} C_q(t) \mathrm{d}t \tag{21}$$

While both unthermostatted and thermostatted XLMD methods are able to qualitatively reproduce the charge distribution generated by CG, Figure 3a shows that the increase of the latent charge temperature for C-XLMD has caused a more noticeable dispersion for the real charges, while the real charge dispersion is better controlled through the Langevin thermostat for SC-XLMD. This is also evident in Figure 3b which shows that the increase of the latent charge temperature using C-XLMD has given rise to an accelerated decorrelation of real charges compared to the CG results. The SC-XLMD using Langevin thermostats slows down the latent momenta and better recovers the auto-correlation behavior at the first several frequencies.

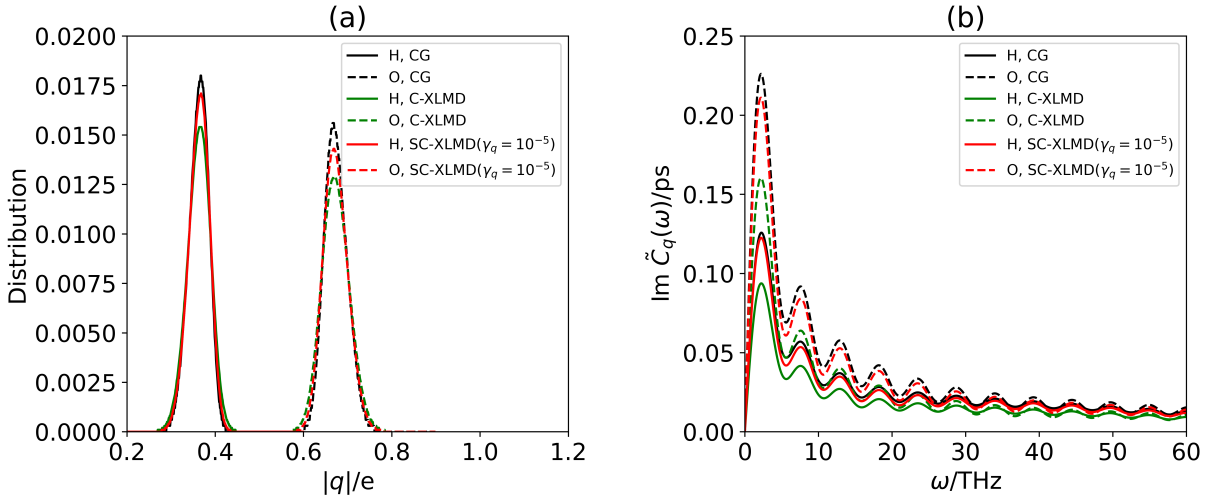

Figure 3: Fluctuating charge properties of water calculated from 500 ps trajectories. (a) Charge distribution function for CG (10^{-10} convergence criteria), C-XLMD, and SC-XLMD with $\gamma_q = 10^{-5}$. (b) The corresponding charge autocorrelation function in the frequency domain for the three methods.

Transport Properties. The recommended scheme, SC-XLMD with $\gamma_q = 10^{-5}$, is now tested for reproduction of dynamic properties and compared to CG. In the NVE ensemble, the mean squared displacement (MSD) as a function of time, and subsequently the diffusion constant calculated from the MSD, is found to be in good agreement with CG (Figure 4a). The accurate description of fluctuating charges using SC-XLMD also provides a solid basis for predicting reactive transport properties such as proton hopping in bulk water as shown in Figure 4b, as measured by its very good consistency with CG.

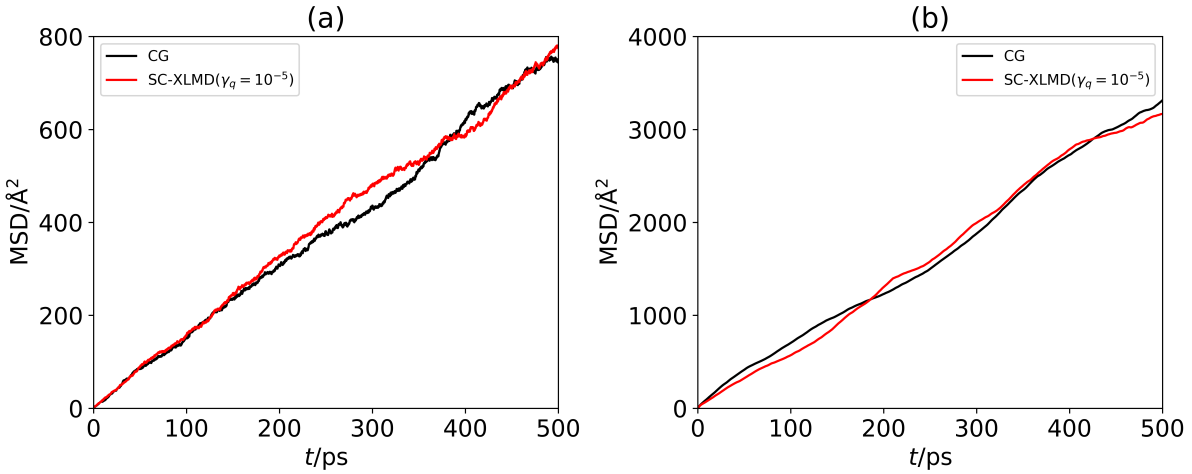

Figure 4: Comparison of methods for transport properties of the CEM solution for bulk water. (a) Diffusion coefficient obtained by SC-XLMD (2.52×10^{-9} m^2 s^{-1}) is in accord with CG (2.51×10^{-9} m^2 s^{-1}) calculated from a 500 ps trajectory. (b) The proton diffusion coefficient obtained by SC-XLMD (1.12×10^{-9} m^2 s^{-1}) is in accord with CG (1.10×10^{-9} m^2 s^{-1}) calculated from a 1 ns trajectory.

Thermodynamic Properties. In addition to the NVE simulations of water and RDX, an NVT simulation is also carried out under 300 K for both systems, and 1000 K for RDX as well. As shown in Figure 5a and 5d for water and RDX, respectively, SC-XLMD provides the same thermal fluctuation behavior of the potential energy as that obtained by CG. We further consider structural properties, i.e. the radial distribution function between oxygen atoms (Figure 5b) as well as between oxygen atom and hydrogen atom (Figure 5c) from SC-XLMD show excellent agreement with CG for water. The two radial distribution functions that involve atoms near the reactive center of RDX, g_{NN} (Figure 5e) and g_{NO} (Figure 5f), show

that the SC-XLMD method also reproduces the radial distribution function using CG-SCF almost perfectly in both cases.

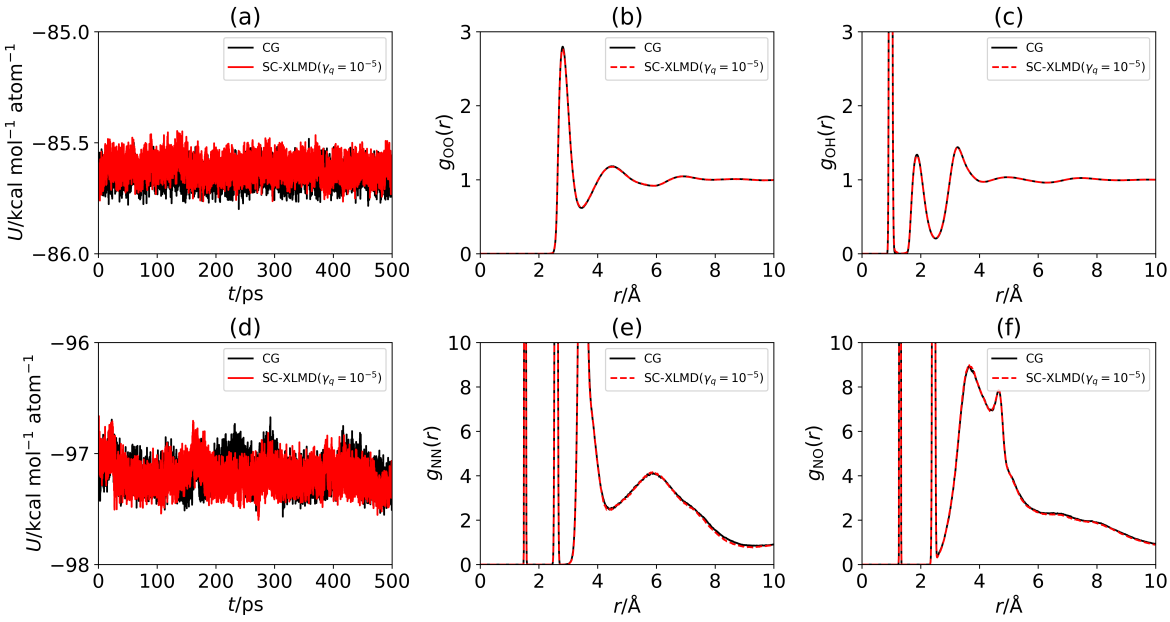

Figure 5: Comparison of CG and SC-XLMD for energy and structural properties in the NVT ensemble for water and RDX. (a) Potential energy from SC-XLMD ($U = -85.61 \pm 0.04$ kcal mol^{-1} atom^{-1}) is in excellent accord with CG ($U = -85.64 \pm 0.04$ kcal mol^{-1} atom^{-1}). Radial distribution functions between (b) oxygen atoms and (c) oxygen and hydrogen atoms for water. (d) The potential energy obtained from CG (-97.18 ± 0.12 kcal mol^{-1} atom^{-1}) and SC-XLMD (-97.20 ± 0.12 kcal mol^{-1} atom^{-1}) for RDX. Radial distribution function between (e) nitrogen atoms and (f) nitrogen and oxygen atoms for RDX.

Benchmarks. Finally, we show that the iteration-free extended dynamics offers significant computational cost advantages over the standard CG-SCF method. We have previously shown that ~40 iterations are required to reach convergence at each timestep for the water system illustrated here, and the iEL/SCF procedure we developed previously[21] for CEM was able to reduce this to ~20 SCF cycles. The SC-XLMD method, by eliminating SCF cycles altogether, is found to perform uniformly well for two types of computational benchmarks where a variety of number of cores (Table 1b) and a variety of system size (Table 1b). Due to the facts for SC-XLMD that (1) there are less communication between processors to exchange the information of charges and (2) the matrix-vector multiplication is significantly reduced,

our implementation of the SC-XLMD approach should benefit even more with the recent optimized software implementations of LAMMPS on many-core hardware architectures.[13,14]

Table 1: The computational scaling of SC-XLMD compared to CG as demonstrated by (a) different number of CPU cores, N_{cores}, and (b) for different sizes as indicated by number of molecules, N_{mlcs}, of the ReaxFF bulk water system, showing the time cost in hours/ns calculated from the "Modify" component of a LAMMPS simulation time analysis where charges and forces are updated.

N_{core}	CG(10^{-8})	CG(10^{-12})	SC-XLMD
1	19.73	26.83	11.16
2	11.42	15.88	6.32
4	7.48	10.38	3.85
8	5.19	7.66	2.47
16	3.62	5.24	1.64
N_{mlcs}	CG(10^{-8})	CG(10^{-12})	SC-XLMD
233	3.62	5.24	1.64
466	5.53	7.99	2.70
932	9.55	13.83	4.75
1864	17.66	25.08	8.29
3728	32.68	45.55	16.39
7456	62.21	89.45	31.47
14912	120.08	169.80	60.14

5 Conclusion

The extended Lagrangian approach that eliminates the self-consistent field step for polarization, iEL/0-SCF, has been extended to charge equilibration models that require the solution of two sets of linear equations for the charges under the constraint of charge conservation. By creating two latent variables of charges and chemical potential under stochastic thermodynamic control, and solving the XLMD with a holonomic constraint that preserves charge conservation, the resulting SC-XLMD is stable and maintains desired accuracy, and yields significant computational speed-ups relative to a standard SCF solver implemented in the reference program LAMMPS. With no SCF cycles to consider, the solution for the many-

body CEM forces is now commensurate with the cost of two-body fixed charge calculations, opening up ReaxFF calculations to much larger systems and longer timescales than previously possible.

The successful formulation and application of SC-XLMD also suggests that SCF-less solutions are widely applicable to more many-body models. We have asserted previously that the iEL/0-SCF method yields satisfactory result because the characteristic decorrelation time τ for polarizable force field model is ~500 times larger than the time step, thus the iEL/0-SCF method is effectively doing SCF iterations on-the-fly. However for CEM this ratio is reduced by an order of magnitude, and yet we have shown here that an SCF-less solution is still viable for CEM using the SC-XLMD method. We thus look forward to reporting more SCF-less solutions for many-body potentials such as *ab initio* molecular dynamics, where the characteristic decorrelation time is similar to the CEM (i.e., ~10 fs).

Acknowledgement

S. T. thanks the University of California Education Aboard Program (UCEAP) for financial and visa support. This work was supported by the U.S. Department of Energy, Office of Science, Office of Advanced Scientific Computing Research, Scientific Discovery through Advanced Computing (SciDAC) program (S.T., I.L., L.L., T.H-G.). The development of the stochastic extended Lagrangian method was partly supported by the National Science Foundation under grant DMS-1652330 (D.A. and L.L.). The authors thank NERSC for computational resources. We thank S.Y. Cheng for discussions.

References

(1) Mortier, W. J.; Ghosh, S. K.; Shankar, S. Electronegativity Equalization Method for the Calculation of Atomic Charges in Molecules.pdf. *Journal of American Chemistry Society* **1986**, *1986*, 4315–4320.

(2) Mortier, W. J.; Genechten, K. V.; Gasteiger, J. Electronegativity Equalization: Application and Parametrization. *J. Amer. Chem. Soc.* **1985**, *107*, 829–835.

(3) Rappé, A. K.; III, W. A. G. Charge Equilibration for Molecular Dynamics Simulations. *Journal of Physical Chemistry* **1991**, *1991*, 3358–3363.

(4) Parr, R. G.; Pearson, R. G. Absolute hardness: companion parameter to absolute electronegativity. *J. Amer. Chem. Soc.* **1983**, *105*, 7512–7516.

(5) Patel, S.; Brooks, C. L. CHARMM fluctuating charge force field for proteins: I parameterization and application to bulk organic liquid simulations. *Journal of Computational Chemistry* **2004**, *25*, 1–16.

(6) Bauer, B. A.; Patel, S. Recent applications and developments of charge equilibration force fields for modeling dynamical charges in classical molecular dynamics simulations. *Theo. Chem. Acc.* **2012**, *131*, 1153.

(7) Wilmer, C. E.; Snurr, R. Q. Towards rapid computational screening of metal-organic frameworks for carbon dioxide capture: Calculation of framework charges via charge equilibration. *Chemical Engineering Journal* **2011**, *171*, 775–781.

(8) Wilmer, C. E.; Kim, K. C.; Snurr, R. Q. An extended charge equilibration method. *J. Phys. Chem. Lett.* **2012**, *3*, 2506–2511.

(9) Demiralp, E.; Çağin, T.; Goddard, W. A. Morse Stretch Potential Charge Equilibrium Force Field for Ceramics: Application to the Quartz-Stishovite Phase Transition and to Silica Glass. *Physical Review Letters* **1998**, *82*, 1708–1711.

(10) Pulay, P. Convergence Acceleration of Iterative Sequences. The Case of SCF Iteration. *Chem Phys Lett* **1980**, *73*, 393–398.

(11) Wang, W.; Skeel, R. D. Fast evaluation of polarizable forces. *Journal of Chemical Physics* **2005**, *123*, 164107.

(12) Nakano, A. Parallel multilevel preconditioned conjugate-gradient approach to variable-charge molecular dynamics. *Comp.Phys. Comm.* **1997**, *104*, 59–69.

(13) Aktulga, H.; Fogarty, J.; Pandit, S.; Grama, A. Parallel reactive molecular dynamics: Numerical methods and algorithmic techniques. *Parallel Comp.* **2012**, *38*, 245–259.

(14) Aktulga, H. M.; Knight, C.; Coffman, P.; O'Hearn, K. A.; Shan, T. R.; Jiang, W. Optimizing the performance of reactive molecular dynamics simulations for many-core architectures. *Intl. J. High Perf. Comp. Appl.* **2019**, *33*, 304–321.

(15) van Duin, A. C. T.; Dasgupta, S.; Lorant, F.; Goddard, W. A. ReaxFF: A Reactive Force Field for Hydrocarbons. *J. Phys. Chem. A* **2001**, *105*, 9396–9409.

(16) O'Hearn, K. A.; Alperen, A.; Aktulga, H. M. Performance optimization of reactive molecular dynamics simulations with dynamic charge distribution models on distributed memory platforms. Proceedings of the ACM International Conference on Supercomputing. 2019; pp 150–159.

(17) O'Hearn, K. A.; Alperen, A.; Aktulga, H. M. Fast Solvers for Charge Distribution Models on Shared Memory Platforms. *SIAM Journal on Scientific Computing* **2020**, *42*, C1–C22.

(18) Niklasson, A. M.; Tymczak, C.; Challacombe, M. Time-reversible Born-Oppenheimer molecular dynamics. *Phys. Rev. Lett.* **2006**, *97*, 123001.

(19) Albaugh, A.; Demerdash, O.; Head-Gordon, T. An efficient and stable hybrid extended Lagrangian/self-consistent field scheme for solving classical mutual induction. *J. Chem. Phys.* **2015**, *143*, 174104.

(20) Albaugh, A.; Niklasson, A. M.; Head-Gordon, T. Accurate Classical Polarization Solution with No Self-Consistent Field Iterations. *J. Phys. Chem. Lett.* **2017**, *8*, 1714–1723.

(21) Leven, I.; Head-Gordon, T. Inertial extended-Lagrangian scheme for solving charge equilibration models. *Phys Chem Chem Phys* **2019**, *21*, 18652–18659.

(22) An, D.; Cheng, S. Y.; Head-Gordon, T.; Lin, L.; Lu, J. Convergence of Stochastic-extended Lagrangian molecular dynamics method for polarizable force field simulation. 2019.

(23) Lipparini, F.; Barone, V. Polarizable Force Fields and Polarizable Continuum Model: A Fluctuating Charges/PCM Approach. 1. Theory and Implementation. *Journal of Chemical Theory and Computation* **2011**, *7*, 3711–3724.

(24) Nomura, K.-i.; Small, P. E.; Kalia, R. K.; Nakano, A.; Vashishta, P. An extended-Lagrangian scheme for charge equilibration in reactive molecular dynamics simulations. *Computer Physics Communications* **2015**, *192*, 91–96.

(25) Zhang, Z.; Liu, X.; Yan, K.; Tuckerman, M. E.; Liu, J. Unified Efficient Thermostat Scheme for the Canonical Ensemble with Holonomic or Isokinetic Constraints via Molecular Dynamics. *The Journal of Physical Chemistry A* **2019**, *123*, 6056–6079.

(26) Plimpton, S. Fast Parallel Algorithms for Short-Range Molecular Dynamics. *J. Comp. Phys.* **1995**, *117*, 1–19.

(27) Li, Y.; Nomura, K.-I.; Insley, J. A.; Morozov, V.; Kumaran, K.; Romero, N. A.; Goddard, W. A.; Kalia, R. K.; Nakano, A.; Vashishta, P. Scalable Reactive Molecular Dynamics Simulations for Computational Synthesis. *Computing in Science and Engineering* **2019**, *21*, 64–75.

(28) Rick, S. W.; Stuart, S. J.; Berne, B. J. Dynamical fluctuating charge force fields: Application to liquid water. *The Journal of Chemical Physics* **1994**, *101*, 6141–6156.

(29) Li, D.-z.; Chen, Z.-f.; Zhang, Z.-j.; Liu, J. Understanding Molecular Dynamics with

Stochastic Processes via Real or Virtual Dynamics. *Chinese Journal of Chemical Physics* **2017**, *30*, 735–760.

(30) Niklasson, A. M. N. Extended Born-Oppenheimer Molecular Dynamics. *Phys. Rev. Lett.* **2008**, *100*, 123004.

(31) Rahaman, O.; van Duin, A. C. T.; Bryantsev, V. S.; Mueller, J. E.; Solares, S. D.; Goddard, W. A.; Doren, D. J. Development of a ReaxFF Reactive Force Field for Aqueous Chloride and Copper Chloride. *J. Phys. Chem. A* **2010**, *114*, 3556–3568.

(32) Shan, T.-R.; Devine, B. D.; Kemper, T. W.; Sinnott, S. B.; Phillpot, S. R. Charge-optimized many-body potential for the hafnium/hafnium oxide system. *Physical Review B* **2010**, *81*.

(33) Martyna, G. J.; Tuckerman, M. E.; Tobias, D. J.; Klein, M. L. Explicit Reversible Integrators for Extended Systems Dynamics. *Mol. Phys.* **1996**, *87*, 1117–1157.

(34) Furman, D.; Wales, D. J. Transforming the Accuracy and Numerical Stability of ReaxFF Reactive Force Fields. *The Journal of Physical Chemistry Letters* **2019**, *10*, 7215–7223, PMID: 31682448.

A The Stochastic Constrained Thermostat in SC-XLMD

In the SC-XLMD method, a Langevin thermostat is used to control the latent charge temperature. However, direct application of the Langevin thermostat is questionable for CEM since it will perturb the total charge conservation of the system by small amounts of white noise, which does not formally conform to the holonomic constraint. To address this, we add an extra holonomic constraint step after the Langevin thermostat:

1. Apply the Langevin thermostat:

$$\boldsymbol{p}_l \leftarrow e^{\boldsymbol{\Gamma}_l \Delta t} \boldsymbol{p}_l + \sqrt{1 - e^{2\boldsymbol{\Gamma}_l \Delta t}} \sqrt{\boldsymbol{M}_l \boldsymbol{T}_l} \boldsymbol{\xi}$$

   where $\boldsymbol{\xi}$ is a vector consisting of $n+1$-dimensional independent standard normal random variable.

2. Calculate the sum of the latent momenta:

$$\Delta \leftarrow \mathbf{1}^T \boldsymbol{p}_l$$

3. Shift the latent momenta to ensure the charge conservation:

$$\boldsymbol{p}_l \leftarrow \boldsymbol{p}_l - \Delta \mathbf{1}/n$$

Though this extra constraint influences the original white noise and has made it colored to some extent, we note that this influence is of order $O(1/n)$ and should not cause any noticeable problems for any but the smallest systems.

B TOC Graphic